Electronic supplementary information (ESI)

Porous cobalt(II)-imidazolate supramolecular isomeric frameworks with selective gas sorption property

Shui-Sheng Chen,[a,c] Min Chen,[a] Satoshi Takamizawa,[b] Peng Wang,[a] Gao-Chao Lv[a] and Wei-Yin Sun*[a]

[a] *Coordination Chemistry Institute, State Key Laboratory of Coordination Chemistry, School of Chemistry and Chemical Engineering, Nanjing National Laboratory of Microstructures, Nanjing University, Nanjing 210093, China.*

E-mail: sunwy@nju.edu.cn; Fax: +86 25 83314502

[b] *Graduate School of Nanobioscience, Yokohama City University, Kanazawa-ku, Yokohama, Kanagawa 236-0027, Japan*

[c] *School of Chemistry and Chemical Engineering, Fuyang Teachers College, Fuyang 236041, China*

Materials and methods. All commercially available chemicals are of reagent grade and were used as received without further purification. The ligand H_3L was prepared according to the reported procedure.[S1] Elemental analyses of C, H and N were taken on a Perkin-Elmer 240C elemental analyzer at the analysis center of Nanjing University. Infrared spectra (IR) were recorded on a Bruker Vector22 FT-IR spectrophotometer by using KBr pellets. Thermogravimetric analyses (TGA) were performed on a simultaneous SDT 2960 thermal analyzer under nitrogen with a heating rate of 10 ºC min^{-1}. Powder X-ray diffraction (PXRD) patterns were measured on a Shimadzu XRD-6000 X-ray diffractometer with Cu Kα (λ = 1.5418 Å) radiation at room temperature. Carbon dioxide (CO_2) and nitrogen (N_2) sorption experiments were carried out on a Belsorp-max volumetric gas sorption instrument

and methane (CH_4) and hydrogen (H_2) sorption experiments were performed on Quantachrome Autosorb-1MP.

X-ray crystallography. The crystallographic data collections for **1** and **2** were carried out on a Bruker Smart Apex CCD area-detector diffractometer with graphite-monochromated Mo Kα radiation (λ = 0.71073 Å) at 293(2) K using ω-scan technique. The diffraction data were integrated by using the *SAINT* program,[S2] which was also used for the intensity corrections for the Lorentz and polarization effects. Semi-empirical absorption correction was applied using the *SADABS* program.[S3] The structures were solved by direct methods and all the non-hydrogen atoms were refined anisotropically on F^2 by the full-matrix least-squares technique using the SHELXL-97 crystallographic software package.[S4]

Reference:

S1 (a) M. P. Castaldi, S. E. Gibson, M. Rudd and A. J. P. White, *Chem. -Eur. J.* 2006, **12**, 138; (b) R. ten Have, M. Huisman, A. Meetsma and A. M. van Leusen, *Tetrahedron*, 1997, **53**, 11355.

S2 S*AINT*, version 6.2; Bruker AXS, Inc., Madison, WI, 2001.

S3 Sheldrick, G. M. *SADABS,* University of Göttingen, Göttingen, Germany.

S4 Sheldrick, G. M. *SHELXTL*, version 6.10; Bruker Analytical X-ray Systems, Madison, WI, 2001.

Table S1 Crystal data and structure refinements for complexes **1** and **2**

	1	**2**
Empirical formula	$C_{18}H_{19}N_7O_2Co$	$C_{15}H_{14}N_6O_2Co$
Formula weight	424.33	369.25
Temperature / K	293(2)	293(2)
Crystal system	Monoclinic	Tetragonal
Space group	$P2_1/c$	$I4_1/a$
a /Å	11.6486(14)	23.3452(10)
b /Å	17.609(2)	23.3452(10)
c /Å	10.5835(13)	14.9359(13)
β /°	110.272(2)	90.00
V (Å^3)	2036.4(4)	8140.0(9)
Z	4	16
Dcalc / (g cm^{-3})	1.384	1.205
F(000)	876	3024
θ range /°	1.86 - 25.01	2.38 - 25.59
Reflections collected	9952	20908
Independent reflections	3583	3820
Goodness-of-fit on F^2	1.063	1.113
R_1 [$I > 2\sigma(I)$][a]	0.0527	0.0568
wR_2 [$I > 2\sigma(I)$][b]	0.1529	0.1614

[a] $R_1 = \Sigma||F_o| - |F_c||/\Sigma|F_o|$. [b] $wR_2 = |\Sigma w(|F_o|^2 - |F_c|^2)|/\Sigma|w(F_o)^2|^{1/2}$, where $w = 1/[\sigma^2(F_o^2) + (aP)^2 + bP]$. $P = (F_o^2 + 2F_c^2)/3$.

Table S2 Selected bond lengths (Å) and bond angles (º) for complexes **1** and **2**

1			
Co(1)-N(1)	2.016(3)	Co(1)-N(5)#1	1.988(3)
Co(1)-N(6)#2	1.993(3)	Co(1)-N(3)#3	2.002(3)
N(5)#1-Co(1)-N(6)#2	113.15(12)	N(5)#1-Co(1)-N(3)#3	111.93(12)
N(6)#2-Co(1)-N(3)#3	112.54(12)	N(5)#1-Co(1)-N(1)	108.30(12)
N(6)#2-Co(1)-N(1)	106.91(12)	N(3)#3-Co(1)-N(1)	103.32(11)
2			
Co(1)-N(1)#4	1.976(3)	Co(1)-N(3)#5	1.979(3)
Co(1)-N(2)	1.988(3)	Co(1)-N(5)#6	2.010(3)
N(1)#4-Co(1)-N(3)#5	109.49(12)	N(1)#4-Co(1)-N(2)	115.50(13)
N(3)#5-Co(1)-N(2)	113.30(14)	N(1)#4-Co(1)-N(5)#6	107.91(13)
N(3)#5-Co(1)-N(5)#6	110.78(13)	N(2)-Co(1)-N(5)#6	99.30(13)

Symmetry transformations used to generate equivalent atoms: #1 x+1, y, z, #2 x+1, -y+1/2, z+1/2, #3 -x+1, y-1/2, -z+3/2, #4 -y+3/4, x+1/4, z+1/4, #5 -x+1/2, -y+3/2, -z+1/2, #6 -x+1/2, -y+1, z-1/2.

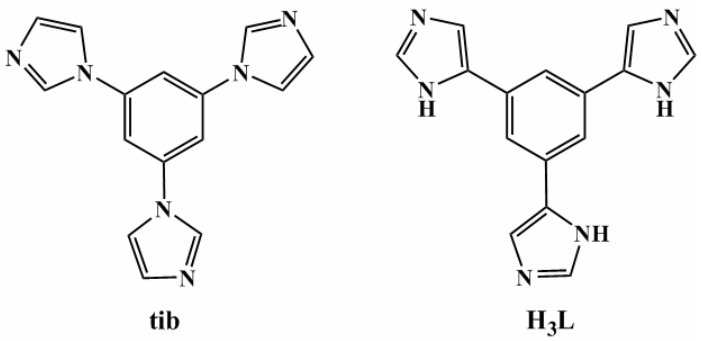

Scheme S1. Schematic structures of tib and H_3L.

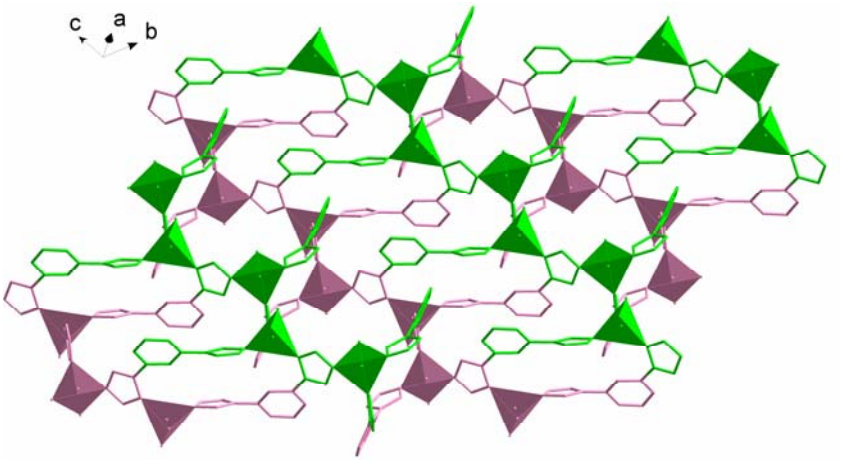

Figure S1. 2D network of **1** formed by two of three imidazole groups of $(HL)^{2-}$ coordinating with Co(II) atoms.

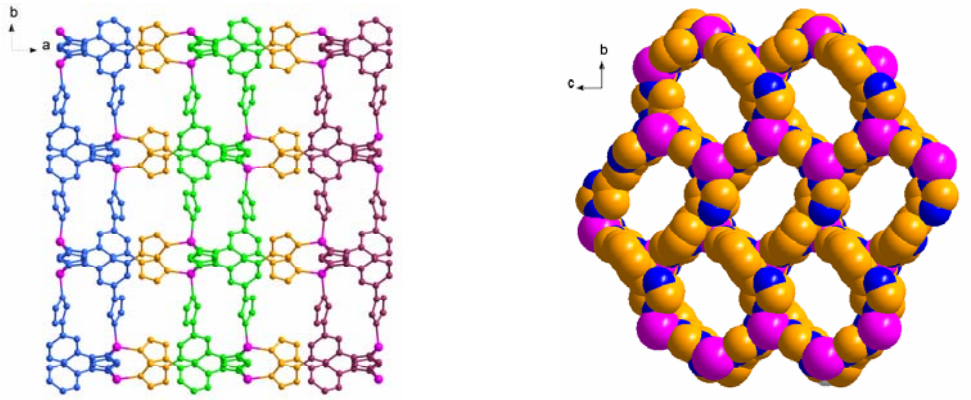

(a) (b)

Figure S2. (a) 3D structure of **1** constructed from the 2D networks (in color) pillared by the third imidazole group (yellow). (b) The space filling view of the 1D channels along *a* axis in **1**.

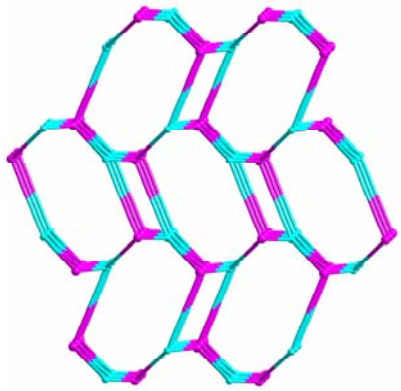

Figure S3. Schematic representation of the zeolite **BCT** topology of **1**, pink balls represent the Co(II) atoms and turquoise balls represent the centers of benzene ring plane of $(HL)^{2-}$.

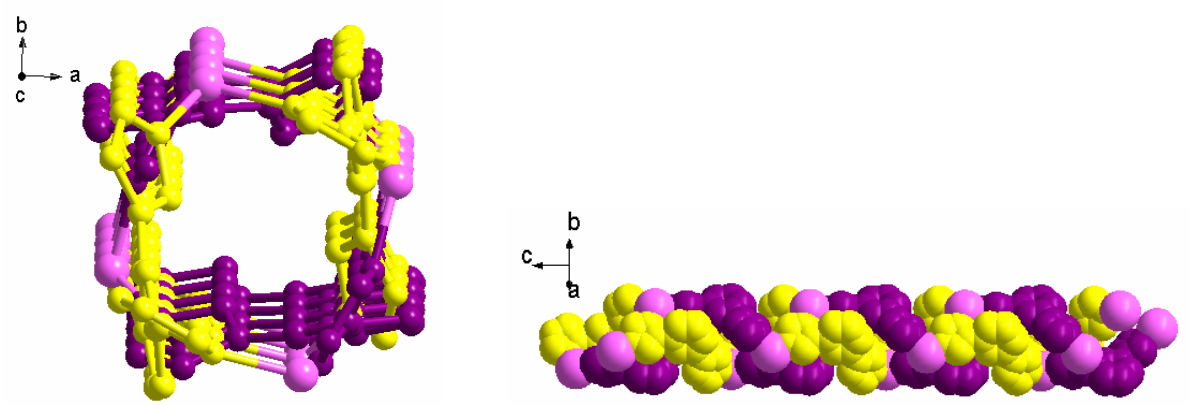

(a) (b)

Figure S4. (a) The helical tubes in **2** represented by central phenyl rings and imidazole groups together with Co(II) atoms. (b) The 4_1 helixes in **2**.

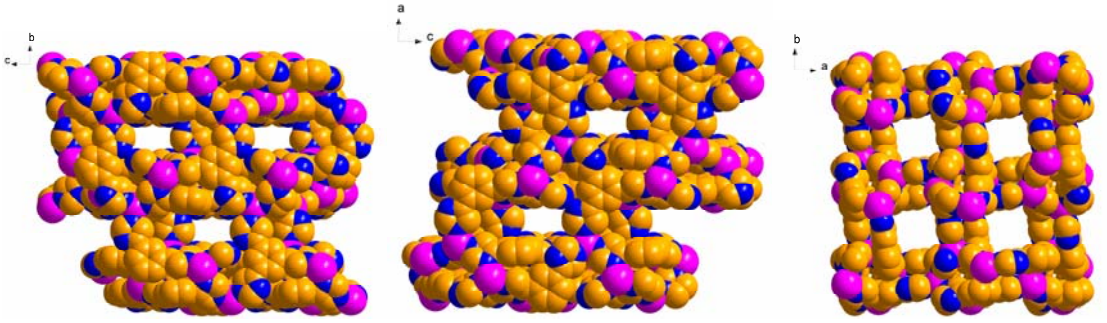

Figure S5. The space filling views of 3D channels of **2** along *a*, *b*, *c* axes respectively.

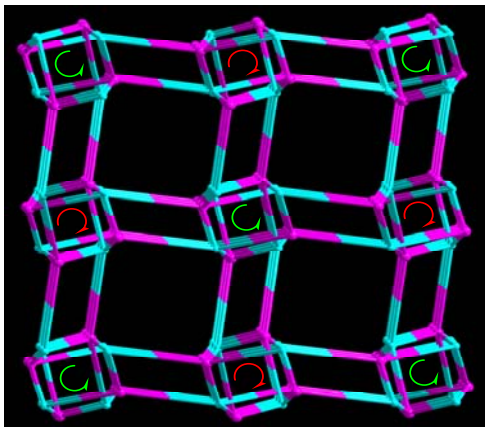

Figure S6. Schematic representation of the **ecl/I** topology of **2**, pink balls represent the Co(II) atoms and turquoise balls represent the centers of benzene ring plane of $(HL)^{2-}$.

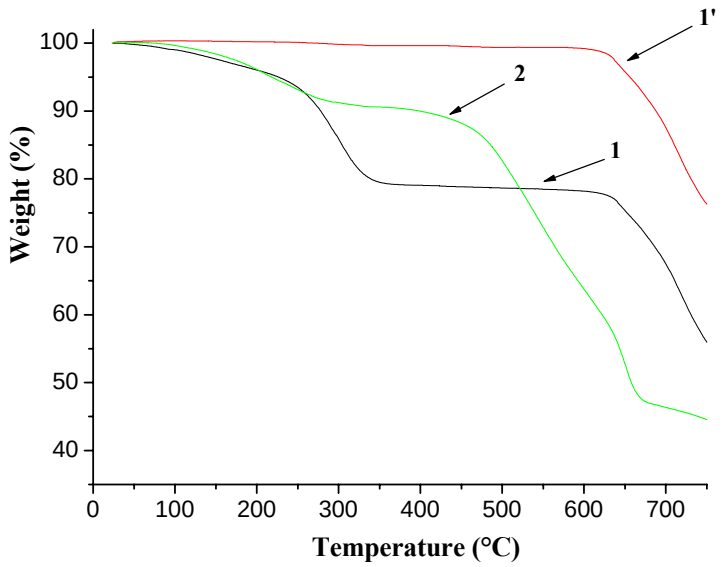

Figure S7. The TGA curves of **1**, **1′** and **2**.

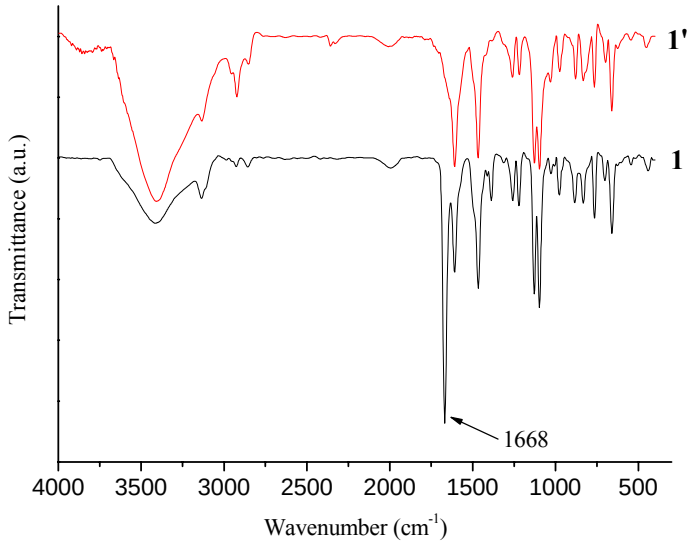

Figure S8. IR spectra of **1** and **1′**.

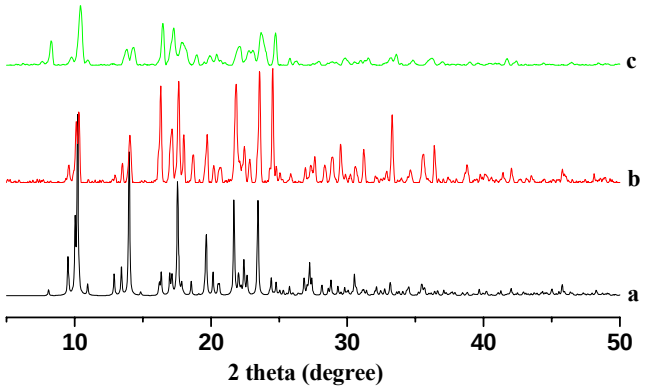

Figure S9. The PXRD patterns of **1**: a - simulated; b - as-synthesized; c - desolvated solid **1′** obtained by heating **1** at 210 ºC under vacuum for 24 h.

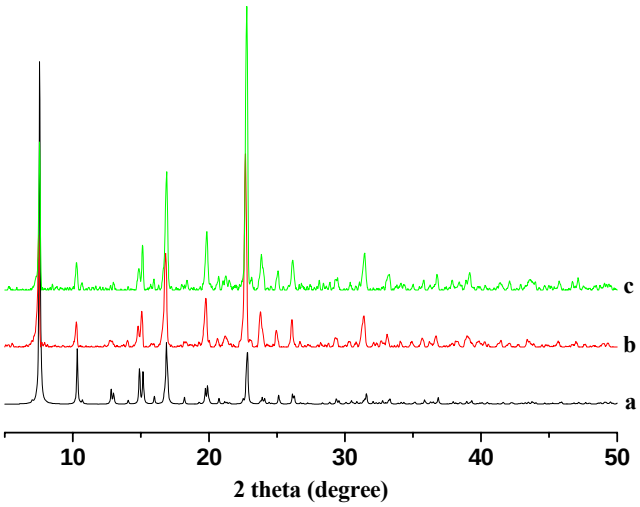

Figure S10. The PXRD patterns of **2**: a - simulated; b - as-synthesized; c - desolvated solid **2′** obtained by heating **2** at 160 ºC under vacuum for 24 h.

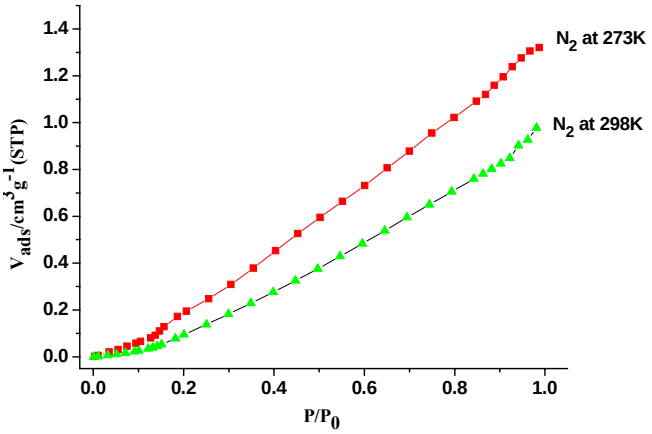

Figure S11. N_2 gas adsorption isotherms of **1′**: (▲) at 298 K, (■) at 273 K. Filled shape: adsorption; open shape: desorption.

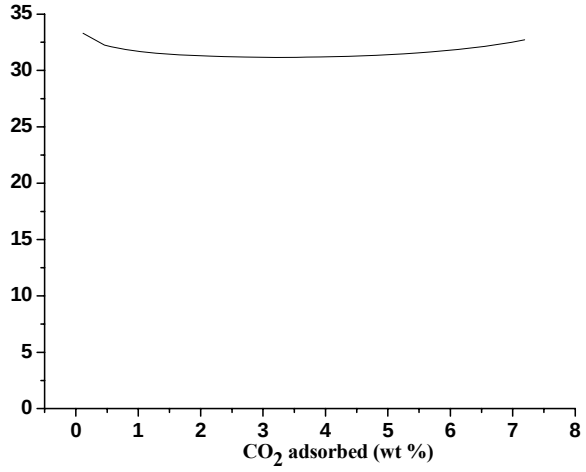

Figure S12. CO_2 adsorption enthalpy for **2′** calculated from the CO_2 adsorption isotherms at 273 and 298 K.

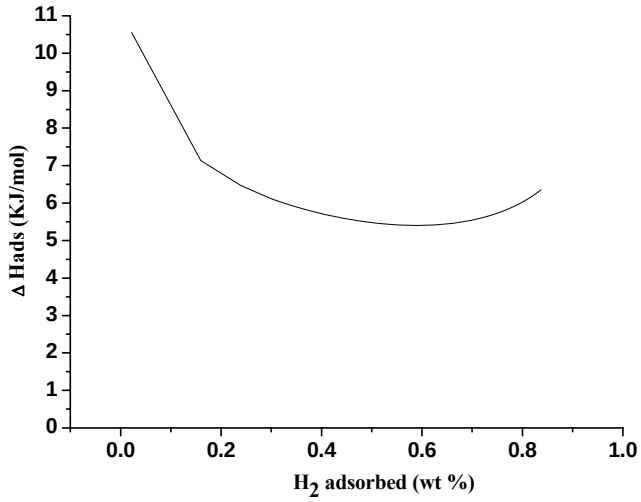

Figure S13. H_2 adsorption enthalpy for **2′** calculated from the H_2 adsorption isotherms at 77 and 87 K.

Analysis of Gas Sorption Isotherms:

The methods are applied to deal with the sorption data according to the literature 15 (*J. Am. Chem. Soc*. 2005, **127**, 9367). The Langmuir-Freundlich equation is used to fit CO_2 and H_2 adsorption isotherms and predict the adsorption capacity of the framework at saturation, and Clausius-Clapeyron equation is employed to calculation the enthalpies of CO_2 and H_2

adsorption.

$$In\left(\frac{P_1}{P_2}\right) = \Delta H_{ads} \times \frac{T_2 - T_1}{RT_1T_2} \qquad (\text{I})$$

Where P_i = pressure for isotherm *i*

T_i = temperature for isotherm *i*

R = 8.315 J / (K·mol)

The equation (I) can be applied to calculate the enthalpy of adsorption of a gas as a function of the quantity of gas adsorbed. Pressure as a function of the amount of gas adsorbed was determined using the Langmuir-Freundlich fit for the isotherms.

$$\frac{Q}{Qm} = \frac{BP^{(1/t)}}{1 + BP^{(1/t)}} \qquad (\text{II})$$

where Q = moles adsorbed

Q_m = moles adsorbed at saturation

P = pressure

B and t are constants

Rearrange (II) to get:

$$P = \left(\frac{Q/Q_m}{B - BQ/Q_m}\right)^t \qquad (\text{III})$$

Replace P in equation (I) to obtain:

$$\Delta H_{ads} = \frac{RT_1T_2}{T_2 - T_1} \times In \frac{\left(\frac{Q/Q_{m1}}{B_1 - B_1Q/Q_{m1}}\right)^t}{\left(\frac{Q/Q_{m2}}{B_2 - B_2Q/Q_{m2}}\right)^t} \qquad (\text{IV})$$

1. Dealing with the carbon dioxide adsorption data in details for 2′:

(1) Fitting CO_2 adsorption isotherms using the Langmuir-Freundlich equation.

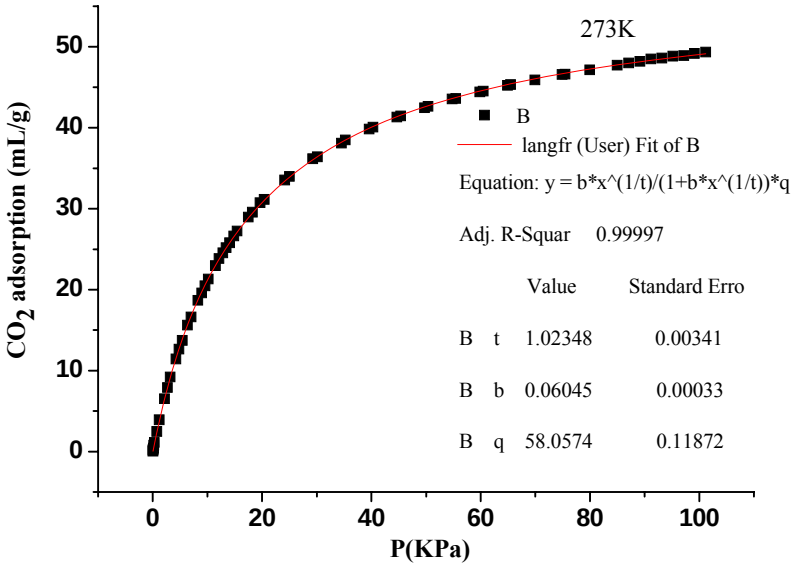

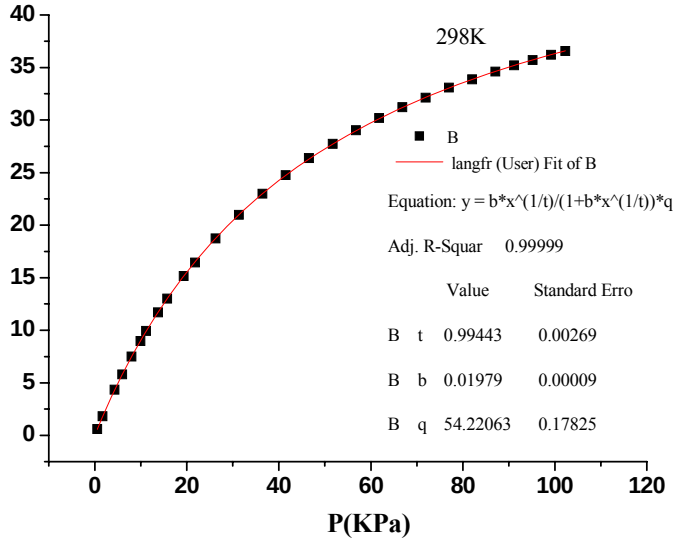

(2) Building the relationship between ln*P* and the quantity of CO_2 adsorbed for the two isotherms by calculating.

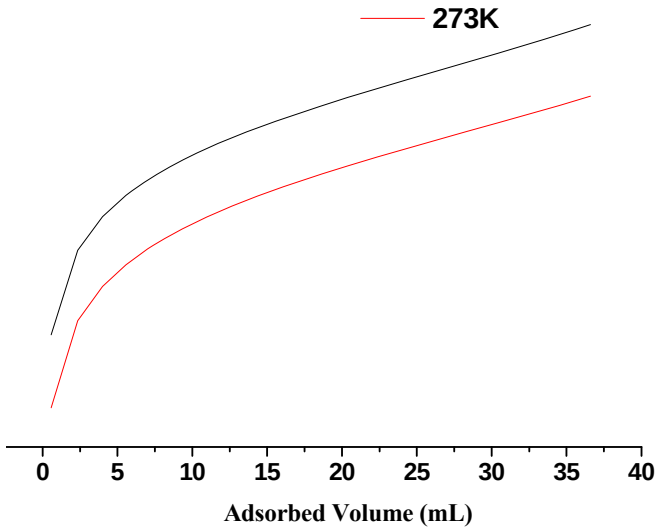

(3) Calculating the $\triangle H_{ads}$ using the equation **IV**.

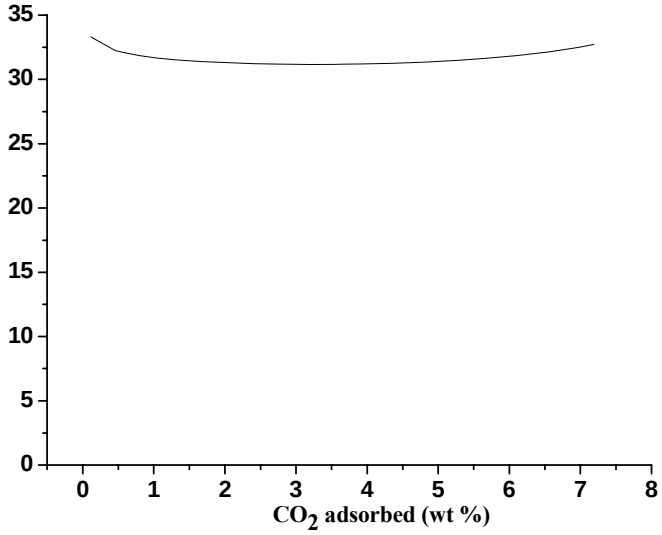

2. Calculation of CO_2/N_2 selectivity

The methods are applied to estimate the CO_2/N_2 selectivity according to the literature 17a (*J. Am. Chem. Soc.*, 2010, **132**, 38). The ratios of these initial slopes of the CO_2 and N_2 adsorption isotherms were applied to estimate the adsorption selectivity for CO_2 over N_2.

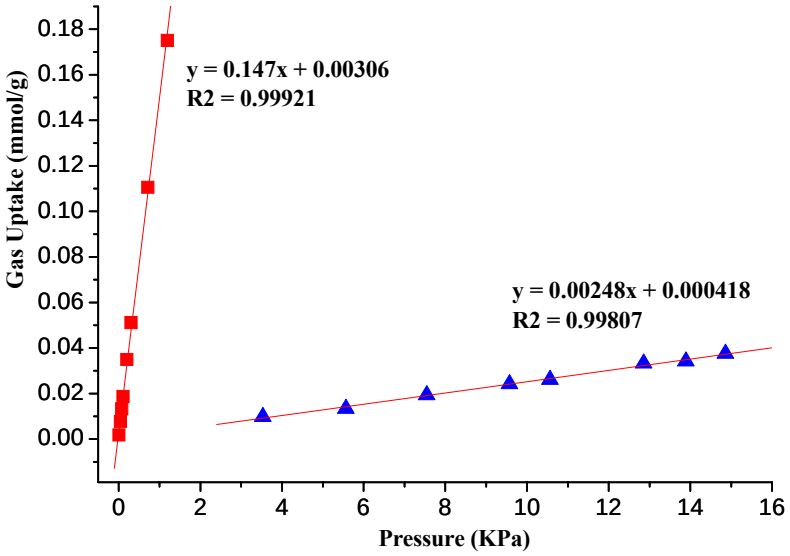

Figure S14. The fitting initial slope for CO_2 and N_2 isotherms collected at 273 K (CO_2: red squares; N_2: blue triangles).

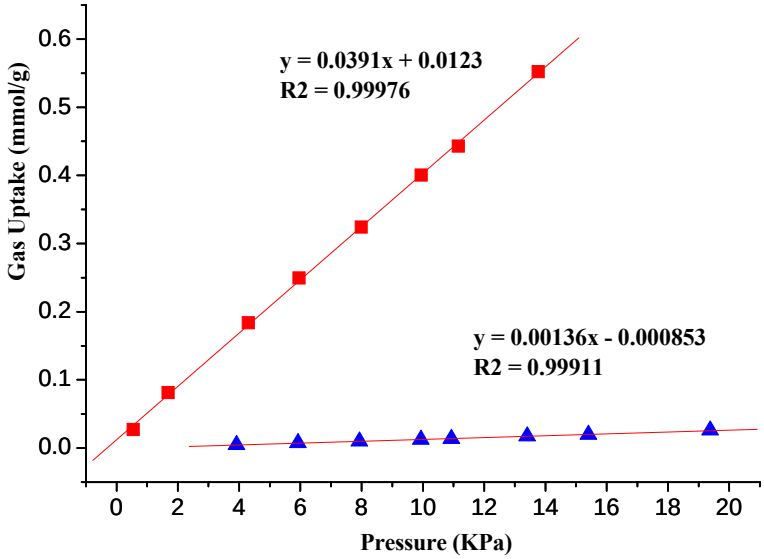

Figure S15. The fitting initial slope for CO_2 and N_2 isotherms collected at 298 K (CO_2: red squares; N_2: blue triangles).

3. Dealing with the hydrogen adsorption data in details:

(1) Fitting H_2 adsorption isotherms using the Langmuir-Freundlich equation.

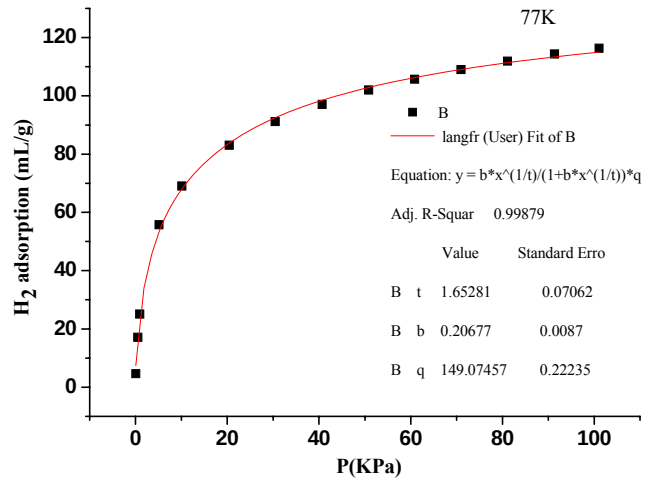

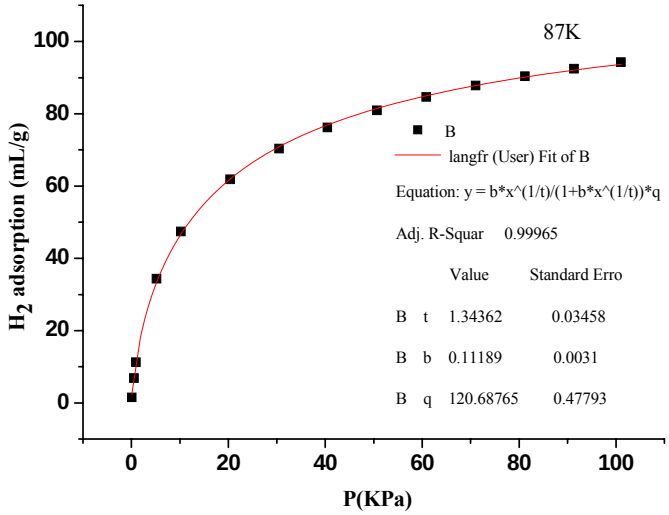

(2) Building the relationship between ln*P* and the quantity of hydrogen adsorbed for the two isotherms by calculating.

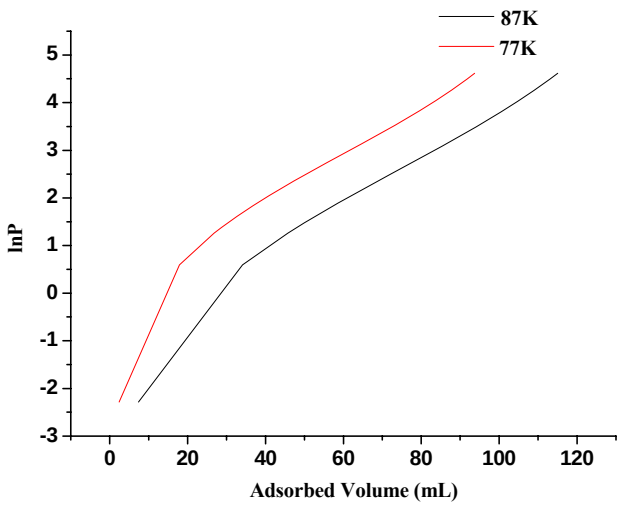

(3) Calculating the $\triangle H_{ads}$ using the equation **IV**.